Counting jumps: does the counting process count?

Laura Ballotta
Bayes Business School (formerly Cass), City, University of London, London, UK

Gianluca Fusai
Università degli Studi del Piemonte Orientale, Novara, Italy
Bayes Business School (formerly Cass), City, University of London, London, UK

Daniele Marazzina*
Politecnico di Milano, Milano, Italy

16th May 2024

Abstract

In this paper, we develop a 'jump diffusion type' financial model based on renewal processes for the discontinuous part of the risk driver, and study its ability to price options and accurately reproduce the corresponding implied volatility surfaces. In this model, the log-returns process displays finite mean and variance, and non-vanishing skewness and excess kurtosis over the long period. The proposed construction is parsimonious, and it allows for a simple and intuitive pricing formula for European vanilla options; furthermore, it offers an efficient Monte Carlo sample path generator for the pricing of exotic options. We illustrate the performance of the proposed framework using observed market data, and we study the features of the best fitting model specifications.

Keywords: Option pricing, Jumps, Counting process, Renewal process, Market calibration

JEL Classification: C51, D52, D53, G12, G13

*Corresponding Author: daniele.marazzina@polimi.it

1 Introduction

The aim of this paper is to develop a jump diffusion model that integrates classical Brownian motion with a 'compound renewal' process, examining its effectiveness in accurately replicating implied volatility surfaces. The log-returns process is expressed as

$$X(t) = \sigma W(t) + \sum_{j=1}^{N(t)} Z_j,$$

where $W(t)$ is a standard Brownian motion, $\sigma > 0$ denotes the diffusion coefficient, $N(t)$ is an independent renewal process, and Z is modelled by a sequence of independent and identically distributed random variables, which are assumed independent of both $W(t)$ and $N(t)$.

The central contribution of this study lies in the investigation of the counting process $N(t)$, with particular focus on the distribution of the inter-arrival times governing $N(t)$. The objective is to circumvent issues related to the convergence to zero over the long period of the skewness and excess kurtosis of the risk neutral distribution of the log-returns.

Traditional financial models based on jump diffusion processes trace back to Merton (1976), and assume that the counting process $N(t)$ is a Poisson process, i.e. the inter-arrival times are exponentially distributed, so that the discontinuous part of the dynamics is modelled by a compound Poisson process. Subsequent developments of this class of processes have been obtained by focusing on the distribution of the jump sizes Z, which in the classical Merton (1976) model are Normal distributed. Thus, we mention Kou (2002) and Cai and Kou (2011) as examples of such developments in which the distributions of choice are respectively the double exponential and the mixed-exponential ones.

However, under the restrictive assumption of a Poisson counting process, such constructions belong to the class of Lévy processes, i.e. processes with independent and stationary increments. Therefore, they are characterized by vanishing skewness and excess kurtosis over long periods of time as a consequence of the central limit theorem, which impacts on the processes ability to fit the implied volatility surface. Indeed, it is documented in Carr and Wu (2003) that the implied volatility smirk in general does not flatten out when maturity increases within the expiry range of traded option contracts. This becomes evident when the implied volatility is plotted against moneyness defined as the logarithm of the strike over the forward, normalised by the square root of maturity. As the downward slope and positive curvature of the implied volatility smirk reflect respectively negative skewness and leptokurtosis in the risk neutral distribution of the log-returns (see Backus *et al.*, 2004, for example), any proposed model should display non-zero skewness and excess kurtosis for increasing maturities, or at best such statistics should decay even more slowly than in the Lévy case.

Two main approaches have been proposed in the literature to capture the persistence of skewness and kurtosis over the long run. The first one is the log-stable model introduced by Carr and Wu (2003), in which by construction the log-returns process exhibits infinite variance and higher-order moments. This design allows the model to deviate from the assumptions of the central limit theorem, and prevents skewness and excess kurtosis to vanish over the long period. However, a log-returns distribution with infinite moments can be inconvenient as it introduces complexities in the statistical analysis and may lead to challenges in model estimation and interpretation. For example, when stock returns have infinite variance, the implied volatility of an option becomes a less reliable measure of future volatility. In such cases, implied volatility may still be calculated, but it may not effectively capture the true level of risk associated with the underlying stock.

A second popular approach is the introduction of stochastic volatility in the return process, as in Heston (1993) for example. Despite their flexibility in capturing the dynamic nature of volatility, often this class of models struggles in fitting the implied volatility of short-term options, due to their inability to generate sufficient probability mass in the tails over these short time horizons.

Our strategy for enhancing jump diffusion models and preventing the flattening of the model implied volatility smirk involves a targeted examination of the counting process $N(t)$, particularly the distribution of its inter-arrival times. As the memoryless property of the exponential distribution is at the origin of the 'Lévy' nature of the (compound) Poisson process, we advocate a broader framework in which inter-arrival times follow distributions beyond the exponential one, and a shift towards the class of renewal processes.

However, as long as the mean and the variance of the inter-arrival times are finite, both the counting process and the compound renewal process are still subject to the central limit theorem, hindering their ability to achieve the desired skewness and excess kurtosis long term characteristics. We address this issue by modelling the inter-arrival times using the Mittag-Leffler distribution (see Pillai, 1990, Jose and Abraham, 2011, for example) and its generalization proposed by Cahoy and Polito (2013), which exhibit infinite moments of all orders, thus evading the central limit theorem's effects.

The proposed approach presents advantages compared to both the log-stable model of Carr and Wu (2003) and the general class of stochastic volatility models. Indeed, in our setup the log-returns distribution retains finite moments thanks to the properties of renewal processes, which is in direct contrast with the approach of Carr and Wu (2003). Furthermore, the model is capable of generating sufficient skewness and excess kurtosis over both short and long terms, guaranteeing in this way a satisfactory fit to the volatility surface for both short and long maturities.

In this paper, we also focus on the issue of duration dependence modelling, whereby duration dependence we refer to how the occurrence of an event in one period influence its subsequent occurrences. By departing from the exponential distribution, we allow the inter-arrival times to show either over or under dispersion, i.e. higher or lower variability compared to the exponential distribution. These features reflect different regimes of duration dependence for the counting process $N(t)$. This deliberate modelling choice enhances flexibility in capturing market dynamics.

An additional contribution of this paper is the adoption of numerical schemes based on the Hilbert transform (see Feng and Linetsky, 2008, Xue *et al.*, 2013, Fusai *et al.*, 2016, for example) to recover relevant probability densities and moments of interest of the counting process. This allows us to move away from renewal equations generally used in reliability theory, and make both option pricing and Monte Carlo simulation accessible for any combination of distributions for inter-arrival times and price revisions, as long as the corresponding characteristic functions are known (we note in this regard that option pricing based on renewal equations has been explored by Montero, 2008). Thanks to this efficient infrastructure, our paper makes a novel contribution in assessing the empirical performance of models incorporating renewal processes in reproducing market implied volatilities.

In this regards, we observe that by assuming price revisions which are independent of the inter-arrival times and are Gaussian distributed, a simple and intuitive analytical formula for European vanilla option prices can be derived. This result also establishes analytically the link between the log-returns volatility and the flow of information measured by transaction volume argued by Ross (1989) and Jones *et al.* (1994) amongst others.

The results from our analysis based on market quotes for options on a number of equity indices point towards a construction catering for both a Brownian motion, and a renewal process with inter-arrival distribution capable of capturing under-dispersion, i.e. a situation in which the business time flows at a more regular pace than postulated by the exponential distribution.

We conclude this Introduction with a brief review of the literature closely related to this topic. Renewal processes, or equivalently continuous time random walks with time intervals between successive steps modelled by random variables, can be interpreted as stochastic volatility models in which both stock returns and variances are influenced by the duration between trades. Already advocated by Clark (1973), models with trades occurring on the basis of a stochastic clock which captures business time have found empirical evidence for ultra high-frequency equity data in Engle and Russell (1998) and Engle (2000) amongst others. Such models have evolved in the literature primarily along two directions.

The first one links directly to the work of Clark (1973) and started with subordinated Brownian motions (i.e. a Brownian motion evolving on a time scale governed by a non-negative Lévy process, that is a subordinator), such as the hyperbolic Lévy process of Eberlein and Keller (1995) and Eberlein *et al.* (1998), the Variance gamma process of Madan *et al.* (1998), and the Normal inverse Gaussian process of Barndorff-Nielsen (1997). This strand of literature has then been extended to the more general setting of time changed Lévy processes by Carr *et al.* (2003), Carr and Wu (2004), Huang and Wu (2004), Ballotta and Rayée (2022) and Ballotta *et al.* (2023). These models present known characteristic functions for the key quantities of interest and therefore allow for the adoption of Fourier transform based methods for option pricing (see Eberlein *et al.*, 2010, for example).

The second direction of this literature focuses instead on renewal processes/continuous time random walks, so that the modelling attention is shifted from the stochastic clock to its pace, i.e. the inter-arrival times between trades, also referred to as duration. The use of these processes in finance has been pioneered by Scalas *et al.* (2000) and Mainardi *et al.* (2000) with the aim of capturing microstructural price features exhibited by high-frequency financial time series, such as memory effects and trade idle times. Option pricing with these processes has been addressed by Cartea and Meyer-Brandis (2009), Cartea (2013) and more recently Jacquier and Torricelli (2020) amongst others. We note a common denominator between Mainardi *et al.* (2000), Cartea and Meyer-Brandis (2009) and Cartea (2013) which is the adoption of the Mittag-Leffler distribution (see Pillai, 1990, Jose and Abraham, 2011, for example) to capture the inter-arrival times. Option pricing is still amenable under the assumption of independence between duration and the price change at the time of trade, also referred to as price revision, as plain vanilla contracts can be priced exploiting Fourier transform based methods (see Cartea and Meyer-Brandis, 2009, Cartea, 2013, Jacquier and Torricelli, 2020, for details).

The paper is organised as follows. In section 2, we introduce renewal processes and study their properties in light of financial applications, together with the necessary numerical schemes for their practical implementation. In section 3, we develop the financial model and derive a useful option pricing formula. The calibration performance of the model is analysed in section 4, and section 5 offers some concluding remarks.

2 Background: Renewal processes

In this section, we introduce renewal processes by reviewing the fundamental definitions, results and properties which play an important role in the construction of the financial models, such as duration dependence and asymptotic behaviour of the higher order cumulants.

2.1 Definitions and general facts

Let $(\Omega, \mathcal{F}, \{\mathcal{F}_t\}_{t\geq 0}, \mathbb{P})$ be a filtered probability space; as in this paper we focus on option pricing, $\mathbb{P}$ denotes a risk neutral probability measure[1]. Let $\{T_j\}_{j\geq 1}$ be a sequence of non-negative i.i.d. random variables with cumulative distribution function (CDF) $F(t) = \mathbb{P}(T_j \leq t)$ modelling the inter-arrival times. The renewal sequence, representing the waiting time till the n-th event, is then given by

$$S_n = \sum_{j=1}^{n} T_j,$$

and the associated renewal counting process is

$$N(t) = \sup\{n \geq 0 : S_n \leq t\} = \sum_{n=1}^{\infty} \mathbb{1}_{S_n \leq t},$$

which has finite moments of all orders (see for example Gut, 1988, Theorem 3.1).

In the context of modelling financial (log-) returns, the sequence $\{T_j\}_{j\geq 1}$ could be interpreted as the time between trades, and consequently the sequence $S_1, S_2, \ldots$ can be interpreted as the times at which a transaction takes place. In other words, the process S_n can be seen as a stochastic clock governing business time, whilst the inter-arrival times would capture the pace at which the clock runs. The renewal process $N(t)$ returns the total number of trades occurred in the interval $(0, t]$.

It follows that the distribution of $N(t)$ is

$$\mathbb{P}(N(t) = n) = F^n(t) - F^{n+1}(t), \tag{1}$$

with $F^n(t)$ denoting the n-th convolution of the distribution of the inter-arrival times, i.e.

$$\begin{aligned} F^n(t) &= \mathbb{P}\left(S_n \leq t\right) \\ &= \mathbb{P}(T_1 + \cdots + T_n \leq t). \end{aligned}$$

Such convolution is in general not known analytically; one exception is the classical case in which the inter-arrival times are exponentially distributed and therefore $N(t)$ is the Poisson process (see Ross, 1970, for example). For all other cases, we resort to numerical schemes based on the Hilbert transform, which we discuss in details in section 2.4.

[1]We note that the proposed market model is incomplete and consequently the risk neutral martingale measure is not unique. Hence, we follow standard practice for incomplete markets and fix the risk neutral measure through the prices of derivative contracts traded in the market.

Finally, in addition to the renewal counting process $N(t)$, we also introduce the 'compound renewal process' (also known in literature as renewal reward process, see Ross, 1970, Sec. 3.9 for example)

$$Y(t) = \sum_{j=1}^{N(t)} Z_j, \tag{2}$$

for Z_j such that $\{(T_j, Z_j) : j \geq 1\}$ are independent and identically distributed pairs of random variables. In the context of our application, we can interpret the reward Z_j as the price revision at time of the trade modelled by the renewal process $N(t)$.

Under the additional assumption of independence between T_j and Z_j, we can express the characteristic function of the compound renewal process as

$$\phi_Y(u;t) = \mathbb{E}\left(\phi_Z(u)^{N(t)}\right) = \sum_{n=0}^{\infty} \phi_Z(u)^n \mathbb{P}(N(t) = n), \tag{3}$$

with $\phi_Z(u)$ denoting the characteristic function of the price revision. With (numerical) knowledge of the distribution of the process $N(t)$, the characteristic function in Equation (3) allows us to recover the probability function of the process $Y(t)$ using appropriate inversion schemes. In this respect, we note that if the sum of the random variables Z_j has known density function then

$$\mathbb{P}(Y(t) \in A) = \sum_{n=0}^{\infty} \mathbb{P}(Y(t) \in A | N(t) = n)\mathbb{P}(N(t) = n), \quad A \in \mathbb{R},$$

and the probability function for the process $Y(t)$ can be recovered with knowledge only of the probability of the counting process $N(t)$.

Given our interest in the statistical features of the relevant distributions, we state the expressions of the cumulants $c_n(\cdot)$ of the process $Y(t)$ which follow from the characteristic function (3) (see Niki *et al.*, 1990, as well).

$$\begin{aligned}
c_1(Y(t)) &= c_1(N(t))c_1(Z) && (4)\\
c_2(Y(t)) &= c_2(N(t))c_1(Z)^2 + c_1(N(t))c_2(Z) && (5)\\
c_3(Y(t)) &= c_3(N(t))c_1(Z)^3 + 3c_2(N(t))c_1(Z)c_2(Z) + c_1(N(t))c_3(Z) && (6)\\
c_4(Y(t)) &= c_4(N(t))c_1(Z)^4 + 6c_3(N(t))c_1(Z)^2c_2(Z) \\
&\quad + c_2(N(t))\left(4c_1(Z)c_3(Z) + 3c_2(Z)^2\right) + c_1(N(t))c_4(Z), && (7)
\end{aligned}$$

with $c_n(N(t))$ denoting the n-th order cumulant of the counting process. Bearing in mind that

$$\begin{aligned}
&\mathbb{E}(Y(t)) = c_1(Y(t)), \quad \mathbb{V}ar(Y(t)) = c_2(Y(t))\\
&\mathbb{E}\left((Y(t) - \mathbb{E}(Y(t)))^3\right) = c_3(Y(t)), \quad \mathbb{E}\left((Y(t) - \mathbb{E}(Y(t)))^4\right) = c_4(Y(t)) + 3c_2(Y(t))^2,
\end{aligned}$$

it follows that the indices of skewness and excess kurtosis are respectively

$$sk(Y(t)) = \frac{c_3(Y(t))}{c_2(Y(t))^{3/2}}, \quad ek(Y(t)) = \frac{c_4(Y(t))}{c_2(Y(t))^2}.$$

The compound renewal process $Y(t)$ can be considered as a generalization of the compound

Poisson process commonly used in the literature (see Merton, 1976, Kou, 2002, Cai and Kou, 2011, for example); however, in general the compound reward process no longer exhibits independent and stationary increments. In other words, the counting process and the corresponding compound renewal process associated to inter-arrival times distributions which are not exponential, no longer belong to the class of Lévy processes. This might have a consequence on the behaviour over time of the higher order moments of these processes; this is an aspect which we will explore in more details in section 2.3.

2.2 Duration dependence

As already noted, in the case in which the inter-arrival times follow the exponential distribution, the resulting renewal process is the Poisson process, i.e. a Lévy process with independent and stationary increments. In all other cases, though, the renewal process is no longer Lévy and therefore the increments show memory. Furthermore, choosing an inter-arrival distribution away from the exponential one allows the modelling of the so-called duration dependence, i.e. the impact that the occurrence of at least one event up to time t has on the probability of a further occurrence in $t + \Delta t$.

As shown in Winkelmann (1995), by choosing a distribution with a varying hazard function

$$h(t) = \frac{F'(t)}{1 - F(t)},$$

we can obtain either negative or positive duration dependence if the hazard function is decreasing or increasing, respectively. Under the assumption of inter-arrival times with monotonic hazard function, Winkelmann (1995) links these properties to the Variance-to-Mean Ratio (VMR) of the renewal counting process $N(t)$

$$VMR = \frac{\mathbb{V}ar(N(t))}{\mathbb{E}(N(t))}.$$

In some more details, negative duration dependence manifests itself for $VMR > 1$, and positive duration dependence is instead achieved for $VMR < 1$. Indeed, $VMR < 1$ implies that the counting process shows a pattern of occurrences which is less random than the one of the Poisson process, given that compared to the expected number of trades the variance is smaller. In other words, the pace of the clock becomes more regular (positive duration dependence), and its distribution is under-dispersed. Overdispersion on the other hand would be associated with clustered distributions (i.e. $VMR > 1$). The exponential distribution, i.e. the Poisson process, leads instead to equi-dispersion.

The above discussion leads to the following considerations. A robust financial model able to reproduce implied volatility surfaces on a daily basis requires an underlying distribution with sufficient flexibility on several features including duration dependence and dispersion.

2.3 Limit theorems and asymptotic behaviour

As mentioned in section 1, our goal is to develop a model for the underlying log-returns which is consistent with the slow decay of skewness and excess kurtosis shown by options implied volatility surfaces. To this purpose, in this section we study the asymptotic behaviour of these statistics for the renewal counting process $N(t)$ and the associated compound renewal process $Y(t)$.

Under typical regularity conditions, the central limit theorem applies to these processes as well, and therefore the asymptotic distribution is normal. This is stated in the following.

Theorem 1 (Central Limit Theorem for Renewal Processes)**.** *Suppose that* $0 < \mathbb{E}(T) < \infty$*,* $\mathbb{V}ar(T) < \infty$*,* $\mathbb{E}|Z| < \infty$ *and* $\mathbb{V}ar(Z) < \infty$*.*

i) For $t \to \infty$

$$N(t) \sim \mathcal{N}\left(\frac{t}{\mathbb{E}(T)}, \frac{\mathbb{V}ar(T)}{\mathbb{E}(T)^3}t\right).$$

ii) For $t \to \infty$

$$Y(t) \sim \mathcal{N}\left(\frac{\mathbb{E}(Z)}{\mathbb{E}(T)}t, \frac{\gamma^2}{\mathbb{E}(T)^3}t\right)$$

for $\gamma^2 = \mathbb{E}(T)^2\mathbb{V}ar(Z) + \mathbb{E}(Z)^2\mathbb{V}ar(T)$*.*

As the inter-arrival times are i.i.d. random variables which are independent of the sequence of i.i.d. random variables Z modelling the rewards, the results follow from Gut (1988), Theorem II.5.2, Theorem IV.2.3 and Remark IV.2.10.

Furthermore, Smith (1959) shows that under the assumption of finiteness of the (raw) moments of the inter-arrival times, the cumulants of the renewal counting process $N(t)$ have a linear asymptotic form in time; consequently, skewness and excess kurtosis of both processes $N(t)$ and $Y(t)$ decay respectively with the reciprocal of the square root of time and the reciprocal of time.

Theorem 1 shows on the one hand that under the assumption of inter-arrival times with finite moments, the associated renewal and compound renewal processes behave asymptotically like Lévy processes. On the other hand, Theorem 1 also shows the path to follow to 'break' the central limit theorem: the renewal model needs to be built out of inter-arrival times distributions with infinite moments, such as the Mittag-Leffler distribution (see for example Pillai, 1990, Jose and Abraham, 2011, Huillet, 2016) and its generalised version (see for example Cahoy and Polito, 2013, Michelitsch and Riascos, 2020, and references therein), which we discuss in some more details in the following. We note in any case that Theorem 3.1 in Gut (1988) guarantees the finiteness of the moments of the counting process $N(t)$ and therefore of the compound renewal process $Y(t)$, independently of the behaviour of the inter-arrival distribution.

The generalised Mittag-Leffler (GML) distribution is described by three parameters $\lambda, \delta > 0$, and $\nu \in (0, 1]$, has density function

$$f(t) = \lambda^\delta t^{\delta\nu-1} E^\delta_{\nu,\delta\nu}(-\lambda t^\nu),$$

and cumulative distribution function

$$F(t) = \lambda^\delta t^{\delta\nu} E^\delta_{\nu,\delta\nu+1}(-\lambda t^\nu),$$

where

$$E^\delta_{\nu,\gamma}(z) = \sum_{k=0}^{\infty} \frac{\delta^{(k)} z^k}{k!\Gamma(\nu k + \gamma)}, \quad \delta, \gamma, z, \nu \in \mathbb{C}, \Re(\nu) > 0,$$

is the generalised Mittag-Leffler function, or Prabhakar function (Prabhakar, 1971), and $x^{(k)}$ is the Pochhammer symbol for the rising factorial, i.e.

$$x^{(k)} = \underbrace{x(x+1)(x+2)\cdots(x+k-1)}_{k \text{ terms}}.$$

The corresponding characteristic function is

$$\phi_T(u) = \left(\frac{\lambda}{\lambda - (\mathrm{i}u)^\nu}\right)^\delta, \tag{8}$$

from which it can be deduced that the finiteness of the moments is only guaranteed for $\nu = 1$.

The above reduces to the Mittag-Leffler (ML) distribution for $\delta = 1$, and the Gamma distribution for $\nu = 1$. If $\delta = \nu = 1$, instead, we recover the exponential distribution. The renewal processes built out of the ML and GML inter-arrival times distributions have been studied in details in Beghin and Orsingher (2010) and Michelitsch and Riascos (2020) amongst others, and are known as (generalised) fractional Poisson processes. The corresponding probability mass function is

$$\mathbb{P}(N(t) = n) = (\lambda t^\nu)^{\delta n} E^{\delta n}_{\nu,\delta n\nu+1}(-\lambda t^\nu) - (\lambda t^\nu)^{\delta(n+1)} E^{\delta(n+1)}_{\nu,\delta(n+1)\nu+1}(-\lambda t^\nu),$$

which follows from (1) and (8) (see also Michelitsch and Riascos, 2020).

For the case of the Mittag-Leffler distribution, i.e. for $\delta = 1$, the following holds (the proof is reported in Appendix A.1).

Proposition 2. *Assume that the inter-arrival times follow a Mittag-Leffler distribution with parameters $\lambda > 0$, $\nu \in (0, 1]$. Let $\mu_k = \mathbb{E}(Z^k)$ and $m_k = \lambda^k \Gamma(1 + k)/\Gamma(1 + \nu k)$.*

i) The first four cumulants of the compound ML renewal process $Y(t)$ are

$$\begin{aligned}
c_1(Y(t)) &= t^\nu \mu_1 m_1 \\
c_2(Y(t)) &= t^{2\nu}\left(m_2 - m_1^2\right)\mu_1^2 + t^\nu \mu_2 m_1 \\
c_3(Y(t)) &= t^{3\nu}\mu_1^3\left(m_3 - 3m_2 m_1 + 2m_1^3\right) + 3t^{2\nu}\mu_2\mu_1(m_2 - m_1^2) + t^\nu \mu_3 m_1 \\
c_4(Y(t)) &= t^{4\nu}\mu_1^4(m_4 - 4m_1 m_3 + 6m_1^2 m_2 - 3m_1^4) + 6t^{3\nu}\mu_1^2\mu_2(m_3 - 2m_1 m_2 + m_1^3) \\
&\quad + t^{2\nu}(4\mu_1\mu_3(m_2 - m_1^2) + 3\mu_2^2 m_2) + t^\nu \mu_4 m_1 - 3c_2(Y(t))^2.
\end{aligned}$$

ii) The asymptotic values for $t \to \infty$ of the indices of skewness and excess kurtosis of the compound ML renewal process $Y(t)$ are

$$\begin{aligned}
sk\,(Y(t)) &= \operatorname{sgn}(\mu_1)\frac{m_3 - 3m_2 m_1 + 2m_1^3}{\left(m_2 - m_1^2\right)^{3/2}} \\
ek\,(Y(t)) &= \frac{m_4 - 4m_1 m_3 + 6m_1^2 m_2 - 3m_1^4}{\left(m_2 - m_1^2\right)^2} - 3.
\end{aligned}$$

iii) For small time horizons, i.e. $t \to 0$, the indices of skewness and excess kurtosis of the *compound ML renewal process* $Y(t)$ *are*

$$\begin{aligned} sk\left(Y(t)\right) &= \frac{\mu_3}{\sqrt{t^{\nu} m_1} \mu_2^{3/2}} \\ ek\left(Y(t)\right) &= \frac{\mu_4}{t^{\nu} m_1 \mu_2^2} - 3. \end{aligned}$$

From Proposition 2 we deduce that over long time horizons the skewness and the excess kurtosis of both the ML renewal and the compound ML renewal processes are non-vanishing, and are controlled only by the parameters of the inter-arrival time distribution, whilst the parameters of the distribution of the revisions Z control only the sign of the skewness of $Y(t)$. Over the short period, instead, skewness and excess kurtosis decay with the reciprocal of powers of time in reasons of the parameter ν, specifically $t^{-\nu/2}$ and $t^{-\nu}$. As $\nu \in (0,1)$, the decay is slower than in the case of renewal processes whose inter-arrival distributions have finite moments. Furthermore, the features of the distribution of the rewards Z play a more incisive role in controlling the distribution of $Y(t)$.

Although for the general case $\delta \neq 1$ analytical expressions for the cumulants of $Y(t)$ are not available, we can still recover them numerically as it will be discussed in section 2.4. Nevertheless, we can gain more precise information about the asymptotic behaviour by means of an application of the Tauberian theorems. In details, it is possible to show on the one hand that the indices of skewness and excess kurtosis of the renewal process and the compound renewal process with GML distributed inter-arrival times converge for $t \to \infty$ to the values derived in Proposition 2, i.e. they share the same asymptotic behaviour as the processes with ML distributed inter-arrival times. On the other hand, over short periods of time, the rate of decay is affected also by the parameter δ, as these statistics decay with rate $t^{-\nu\delta/2}$ and $t^{-\nu\delta}$ respectively (see Appendix A.2 for the full argument). This implies that for $t \to 0$ the speed of convergence is faster in the GML case than in the ML one if $\nu\delta > 1$.

2.4 Numerical schemes for renewal processes

As previously noted, in general the distribution of the renewal counting process $N(t)$ is not known analytically. For this purpose, in this paper, we adopt the Hilbert transform technique, which is commonly used for pricing purposes (see Feng and Linetsky, 2008, Xue *et al.*, 2013, Fusai *et al.*, 2016, for example).

Thus, let $\phi(u)$, $u \in \mathbb{R}$, denote the characteristic function of the distribution of the inter-arrival times, then in virtue of their independence

$$F^n(t) = \frac{1}{2} - \frac{\mathrm{i}}{2}\mathcal{H}(e^{-\mathrm{i}ut}\phi^n(u))(0), \quad \mathrm{i} = \sqrt{-1},$$

(see Feng and Lin, 2013), where $\mathcal{H}f(\cdot)$ denotes the Hilbert transform of the function f and is defined as the Cauchy principal value integral

$$\mathcal{H}f(x) = \frac{1}{\pi} p.v. \int_{\mathbb{R}} \frac{f(u)}{x-u} du.$$

As shown in Feng and Linetsky (2008) and Fusai *et al.* (2016), the Hilbert transform can be efficiently computed exploiting sinc functions.

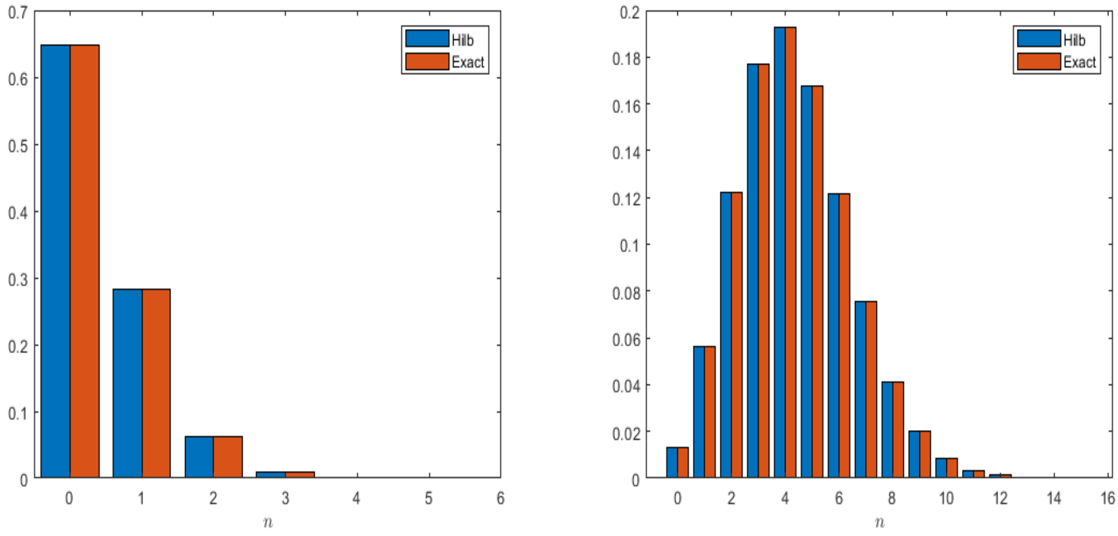

a) Time horizon: 1 year

b) Time horizon: 10 year

Figure 1: Recovering the distribution of $N(t)$: the case of the Poisson process with $\lambda = 0.4352$. Hilbert transform vs exact formula. Time horizons: Panel a) 1 year, Panel b) 10 years.

For illustration purposes, in Figure 1 we show the distribution of a renewal process with exponentially distributed inter-arrival times recovered using the methodology described above. As the resulting counting process is Poisson, we can benchmark the procedure against the known formula of the Poisson probability mass. As Figure 1 confirms, the fit is very accurate.

Access to the distribution of the renewal process $N(t)$ allows us to recover directly the moments, as

$$\mathbb{E}(N(t)^k) = \sum_{n=0}^{\infty} n^k \ \mathbb{P}(N(t) = n), \quad k = 1, 2, \ldots$$

bypassing any related renewal Equation, as well as the characteristic function of the compound renewal process $Y(t)$ given in Equation (3). Moreover, the knowledge of the CDF $F(t)$ permits us to easily simulate the inter-arrival times via the inverse transform method, as shown in Algorithm 1. This is exploited in section 4.2.3 to price barrier options via Monte Carlo simulation.

3 The market model

We model the process driving the stock price as the sum of a Brownian motion and an independent compound renewal process, that is

$$S(t) = S(0)e^{(r-q)t+X(t)-\varpi(t)}, \tag{9}$$

for

$$X(t) = \sigma W(t) + Y(t). \tag{10}$$

In the above specification, $S(0)$ is the spot price, r is the (constant) continuously compounded risk free rate of interest, and q is the dividend yield. Furthermore, $W(t)$ is a standard Brownian motion and $Y(t)$ is the compound renewal process as defined in Equation (2), and assumed independent of $W(t)$. The parameter $\sigma \geq 0$ is the diffusion coefficient, and

$$\varpi(t) = \frac{\sigma^2}{2}t + \ln \phi_Y(-\mathrm{i}; t)$$

is the exponential compensator of $X(t)$, i.e. the risk neutral adjustment ensuring that the discounted asset price is a martingale. Finally, we assume that the price revisions Z (see Equation (2)) are normally distributed with mean $\mu_Z \in \mathbb{R}$ and standard deviation $\sigma_Z > 0$.

The posited general specification includes as a special case the Merton (1976) jump diffusion model, which can be recovered by choosing exponentially distributed inter-arrival times. Thus, we refer to the general construction (10) as compound renewal diffusion process, which differs from the Merton (1976) model in terms of the inter-arrival times distribution. Several choices are possible and discussed in details in the following section.

3.1 Inter-arrival times and model properties

As noted in section 2, we require distributions which are sufficiently flexible to capture the market dynamics implicit in option prices, and features such as implied volatility smirks which do not flatten out as maturities increase up to the observable horizon offered by the option market.

For this purpose, we focus on the performance of the GML distribution for the inter-arrival times. Indeed, as already noted, this distribution generates a compound renewal process $Y(t)$ with non vanishing skeweness and excess kurtosis. Furthermore, as the GML density function is com-

Algorithm 1 Sampling process (10)

```
procedure SIMULATION
    Nsim                                   ▷ Number of simulations
    M                                      ▷ Number of time-steps
    T                                      ▷ Time-horizon
    sigma                                  ▷ Diffusion
  Initialization
    dt=T/M
    t=[0:dt:T]                             ▷ Time grid
    X                                      ▷ Matrix Nsim x M+1 with zeros elements
  Compute the cdf F(t) → F
  for j=1:Nsim do
      tau=0                                ▷ Jump time
      jumptime=[ ]                         ▷ Vector of jump-times
      while tau<T do                       ▷ Countdown simulation
          Sample uniform random number ← u
          Find t such that F(t)=u          ▷ Simulate the interarrival time inverting the cdf
          tau=tau+t
          jumptime=[jumptime tau];
      for k=1:M do
          Sample standard normal random number ← z
          X(j,k+1)=X(j,k)+sigma*sqrt(dt)*z ▷ Sampling continuous part
          for jj=1:length(jumptime)-1 do   ▷ Sampling jump part
              if t(k)<jumptime(jj)<=t(k+1) then
                  Sample from a N(μ_j; σ_J^2) ← Z
                  X(j,k+1)=X(j,k+1)+Z      ▷ Add the jump
```

pletely monotone for $\nu\delta \leq 1$ (see Capelas de Oliveira *et al.*, 2011, for example), the monotonicity of the corresponding hazard function, and therefore the type of duration dependence shown by the renewal process $N(t)$, depends on the combination of the values of the model parameters.

As the GML distribution includes the ML, Gamma and exponential distributions as special cases, in the following we compare the performance of these nested models in terms of reproducing the implied volatility smile observed from market option quotes. In particular, we note the following points. Jose and Abraham (2011) have shown through extensive simulations that the ML distribution is overdispersed for $\nu \in (0, 1)$, and consequently the resulting renewal process has a clustered distribution. Similarly, Yannaros (1988) has shown that the Gamma distribution is overdispersed if $\delta \in (0, 1)$ and under-dispersed otherwise, whilst the exponential distribution is - as already noted - equidispersed.

In addition to the above, we consider also another generalization of the exponential distribution, which is the Weibull distribution, together with some other commonly used distributions for non-negative random variables such as the noncentral chi-squared and the inverse Gaussian ones. Table 1 summarizes the main features of these distributions.

In terms of dispersion properties, we note that the Weibull distributions is under-dispersed for $k > 1$, and overdispersed when $k \in (0, 1)$ (see McShane *et al.*, 2008, Yannaros, 1994), whilst the inverse Gaussian distribution is characterised by a unimodal hazard function, which increases from 0 to its maximum value and then decreases asymptotically to a constant (see Lemeshko *et al.*, 2010, for further details); this implies that it is non-monotonic and therefore the VMR depends on the combination of the values of the distribution's parameters like in the case of the GML distribution. Similar considerations hold for the noncentral chi-squared distribution as well.

Finally, we observe that, with the exception of the ML distribution and its generalised version, the distributions in Table 1 have finite moments. Consequently, Theorem 1 applies and the skewness and excess kurtosis of the associated renewal processes are vanishing over time with decay rate of order $t^{-1/2}$ and t^{-1} respectively. These convergence rates though can be quite slow over the standard horizons given by the traded maturities. This is illustrated in Figure 2 in which we reproduce the behaviour over time of the skewness and excess kurtosis of the compound renewal process $Y(t)$, and the log-returns process $X(t)$ for the case of exponential and ML distributed inter-arrival times. The parameters are chosen so that the renewal counting processes have the same unit time mean, and the price revisions follow the same distribution. Over a 5 years period, which is a time horizon longer than the maturities of the large majority of liquid options, the statistics of these processes are quite far from their corresponding limiting values.

Figure 2 shows also another interesting feature, and it concerns the short time behaviour of these statistics. Whilst the skewness and excess kurtosis over short periods of time of the process $Y(t)$ can reach significant levels, their magnitudes for the process $X(t)$ are always smaller. This feature is observed for all inter-arrival times distributions and it is due to the Brownian motion component, which only contributes to increase, ceteris paribus, the level of the overall variance without affecting the higher order cumulants. Indeed, we obtain from Equation (10) that

$$\begin{aligned} \mathbb{V}ar\left(X(t)\right) &= \sigma^2 t + \mathbb{V}ar\left(Y(t)\right), \\ c_n(X(t)) &= c_n(Y(t)), \quad n \geq 3, \end{aligned}$$

Table 1: Inter-arrival distributions, their characteristic functions and related statistics. A note: the gamma distribution with $\delta = 1$ corresponds to the exponential distribution; the Weibull distribution with $k = 1$ corresponds to the exponential distribution with parameter $1/\lambda$; the Mittag-Leffler distribution with $\nu = 1$ corresponds to the exponential one; the generalised Mittag-Leffler distribution with $\delta = 1$ corresponds to the Mittag-Leffler one; the generalised Mittag-Leffler distribution with $\nu = 1$ corresponds to the gamma one.

Inter-arrival time distribution	Characteristic function $\phi(u) = \mathbb{E}\left(e^{iuT}\right)$	$\mathbb{E}(T)$	$\mathbb{V}ar(T)$
Exponential	$\frac{\lambda}{\lambda - \mathrm{i}u}, \lambda > 0$	$\frac{1}{\lambda}$	$\frac{1}{\lambda^2}$
Gamma	$\left(\frac{\lambda}{\lambda - \mathrm{i}u}\right)^{\delta}, \lambda, \delta > 0$	$\frac{\delta}{\lambda}$	$\frac{\delta}{\lambda^2}$
Weibull	recovered numerically[2] from pdf $\frac{k}{\lambda}\left(\frac{x}{\lambda}\right)^{k-1} \exp\left(-\left(\frac{x}{\lambda}\right)^{k}\right), x \geq 0, \lambda, k > 0$	$\lambda\Gamma\left(1 + \frac{1}{k}\right)$	$\lambda^2\left(\Gamma\left(1 + \frac{2}{k}\right) - \Gamma\left(1 + \frac{1}{k}\right)^2\right)$
Noncentral chi-squared	$\frac{\exp\left(\frac{\mathrm{i}u\lambda}{1-2iu}\right)}{(1 - 2\mathrm{i}u)^{k/2}}, \lambda, k > 0$	$k + \lambda$	$2(k + 2\lambda)$
Inverse Gaussian	$\exp\left(\frac{\lambda}{\mu}\left(1 - \sqrt{1 - 2\mathrm{i}u\frac{\mu^2}{\lambda}}\right)\right), \lambda, \mu > 0$	μ	$\frac{\mu^3}{\lambda}$
Mittag-Leffler (ML)	$\frac{\lambda}{\lambda - (\mathrm{i}u)^{\nu}}, \lambda > 0, \nu \in (0, 1]$	Not defined if $\nu < 1$	Not defined if $\nu < 1$
Generalised Mittag-Leffler (GML)	$\left(\frac{\lambda}{\lambda - (\mathrm{i}u)^{\nu}}\right)^{\delta}, \lambda, \delta > 0, \nu \in (0, 1]$	Not defined if $\nu < 1$	Not defined if $\nu < 1$

[2] If W is distributed as a Weibull, then $W = \lambda X^{1/k}$, where X is distributed as an Exponential of parameter 1. From that we get $\phi(u) = \int_0^{\infty} exp(iu\lambda x^{1/k})exp(-x)dx$ which can be computed as $\sum_{n=0}^{\infty}(-i\lambda u)^n\Gamma(1 + n/k)/\Gamma(1 + n)$, exploiting the Fox H-function. This is stable if $k > 1$, otherwise an asymptotic expansion can be used, see Mathai *et al.* (2009).

where $c_n(\cdot)$ denotes the cumulant of the n-th order. Thus, for short time horizons the diffusion coefficient represents a mechanism to better regulate the skewness and the excess kurtosis of the log-returns distribution.

This tempering effect of the Brownian motion could extend to the asymptotic case for $t \to \infty$, even in the case of inter-arrival times distributions with infinite moments. Indeed, it can be deduced from Proposition 2 and the following discussion in section 2.3 that if the GML parameter ν is less than 0.5, the dominant term in the variance of $X(t)$ is given by the diffusion part, i.e. $\sigma^2 t$. As a consequence, the compound renewal diffusion process $X(t)$ would exhibit vanishing skewness and excess kurtosis.

We conclude this part with the following consideration. As already noted, in the case of the models built on the ML and GML distributions, we stop the central limit theorem by assuming inter-arrival times with infinite moments. Nevertheless, the processes $N(t)$ and $Y(t)$ do have finite moments of all order and so does the log-returns process $X(t)$. This is in contrast with the approach adopted by Carr and Wu (2003) to prevent the 'central limit theorem effect' by modelling the log-returns with a stable process: in their setting, in fact, the log-returns process continues to have infinite variance, although the moments in the spot index level are finite.

3.2 Option pricing

The assumption of normally distributed price revisions allows us to derive a convenient semi-analytical expression for the price of European options, as shown in the following.

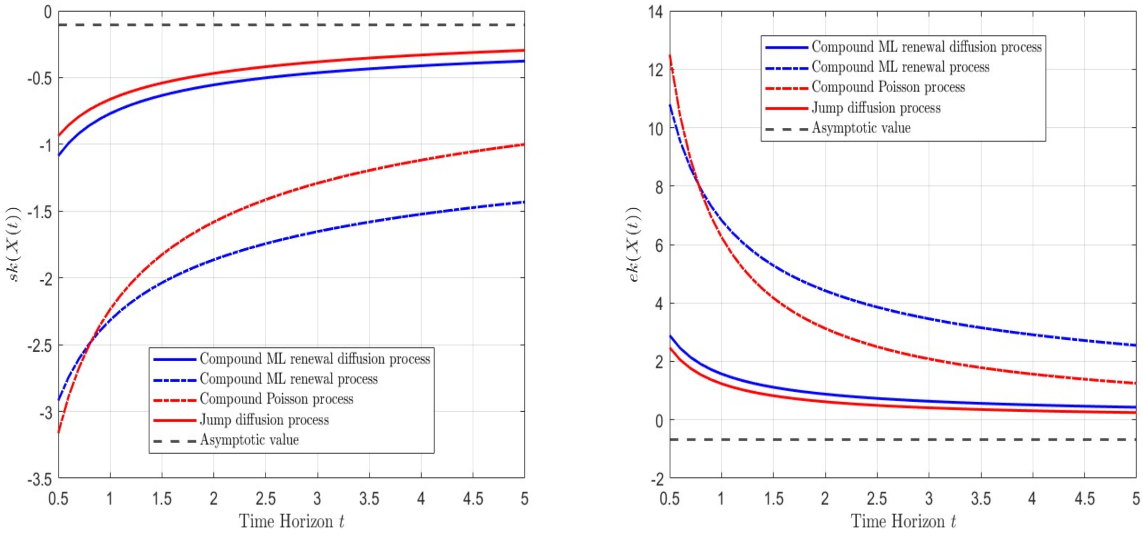

a) Skewness $sk(X(t))$ b) Excess kurtosis $ek(X(t))$

Figure 2: Skewness $sk(\cdot)$ and excess kurtosis $ek(\cdot)$: Merton jump diffusion process vs compound ML renewal diffusion process. Diffusion coefficient: $\sigma = 0.2$. Compound Poisson process with rate of arrival $\lambda = 0.4352$. Compound ML renewal process - parameters: $\lambda = 0.4$, $\nu = 0.75$. Price revisions for both models: $Z \sim \mathcal{N}(-0.2, 0.2^2)$. Asymptotic value: see Proposition 2. Time expressed in years.

Proposition 3. *The price of a European option $C(0)$ struck at K, expiring at T, and written on a stock with dynamics given by Equations (9)–(10) and $Z \sim \mathcal{N}(\mu_Z, \sigma_Z^2)$ is*

$$C(0) = \sum_{n=0}^{\infty} blsprice(S(0), K, r, T, v(n), q(n))\mathbb{P}(N(T) = n), \tag{11}$$

with $blsprice(S(0), K, r, T, v(n), q(n))$ denoting the Black and Scholes (1973) price of a European option written on an underlying asset with volatility

$$v(n) = \sqrt{\sigma^2 + \frac{n}{T}\sigma_Z^2},$$

and dividend yield

$$q(n) = q + \frac{1}{T}\ln \phi_Y(-\mathrm{i}; T) - \frac{n}{T}\left(\mu_Z + \frac{\sigma_Z^2}{2}\right).$$

The proof is reported in Appendix A.3. Formula (11) can be easily extended to compute greeks, as delta Δ and gamma Γ. As an example, $\Delta = \sum_{n=0}^{\infty} blsdelta(S(0), K, r, T, v(n), q(n))\mathbb{P}(N(T) = n)$, with *blsdelta* denoting the Black and Scholes (1973) delta.

The result offered in Proposition 3 is simple to implement and intuitive. Indeed, from the point of view of the practical implementation, the infinite summation in the pricing Equation (11) can be truncated to a value $N_{\max}$ such that

$$\mathbb{P}(N(T) = N_{\max}) < \varepsilon_1,$$

and

$$\sum_{i=0}^{N_{\max}} \mathbb{P}(N(T) = i) \leq 1 - \varepsilon_2.$$

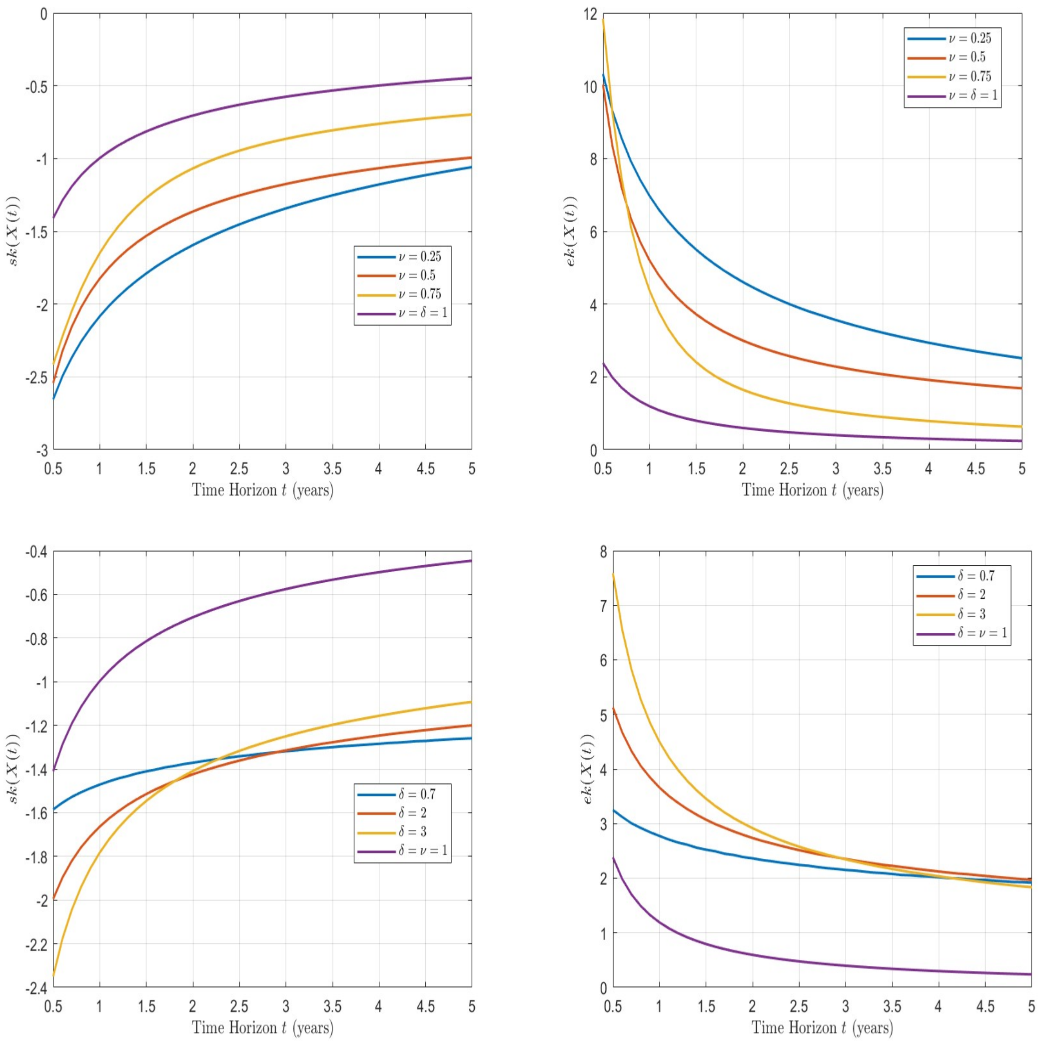

a) Skewness $sk(X(t))$ b) Excess kurtosis $ek(X(t))$

Figure 3: Impact of the GML parameters ν (top panels) and δ (bottom panels) on the skewness (left hand side) and excess kurtosis (right hand side) of the distribution of the compound renewal diffusion process $X(t)$. Parameters: $\sigma = 0.12$, $\mu_Z = -0.3460$, $\sigma_Z = 0.2465$, $\lambda = 1.6166$, $\delta = 3.7803$ (top panels), $\nu = 0.4984$ (bottom panels) - see Table 3, S&P500 case. Time expressed in years.

In our implementation, we set $\varepsilon_1 = 10^{-6}$ and $\varepsilon_2 = 10^{-5}$.

In terms of intuition, we can interpret the option price as an average of Black-Scholes prices across all possible values of the renewal counting process $N(T)$. We pay particular attention to the two inputs of the Black-Scholes formula $q(n)$ and $v(n)$. The former can be read as an adjusted dividend yield.

The term $v(n)$ can be instead interpreted as the (conditional) volatility of the log-returns, which is now stochastic as it depends on the counting process $N(T)$ and its distribution. In the case of the Merton (1976) jump diffusion model, $N(T)$ has independent and stationary increments, thus the structure of this volatility is relatively elementary; in our framework instead this structure is richer and therefore it has the potential for generating realistic implied volatility surfaces. Hence, this construction formalizes the argument of Ross (1989) and Jones *et al.* (1994) that there is a positive relation between the log-returns (implied) volatility and the rate of flow of information, the latter being measured by the number of transactions taking place over any time interval.

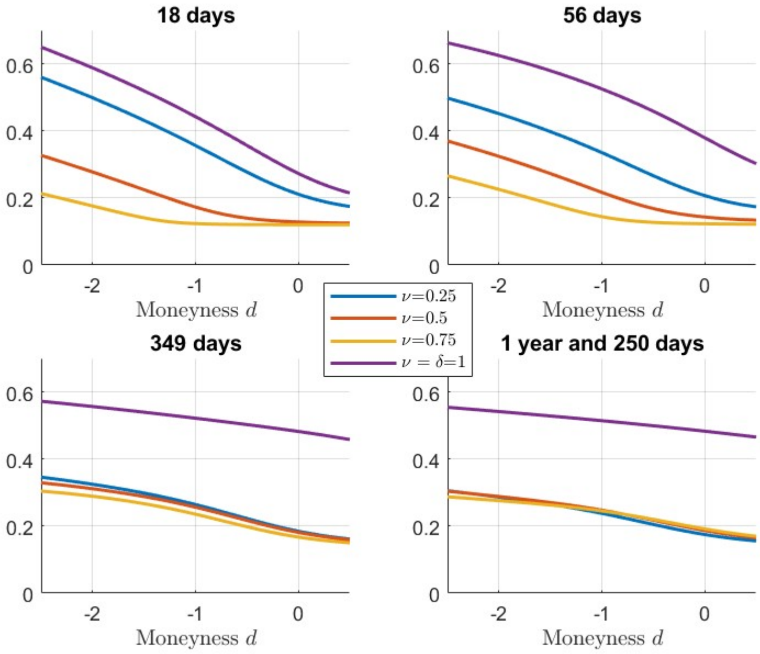

Figure 4: Impact of the parameter ν of the generalized Mittag-Leffler on the implied volatility. All others parameters as in Table 3, S&P500 case. Standardized moneyness: $d = \ln(K/S)/(\sigma_I\sqrt{T})$, as in Foresi and Wu (2005).

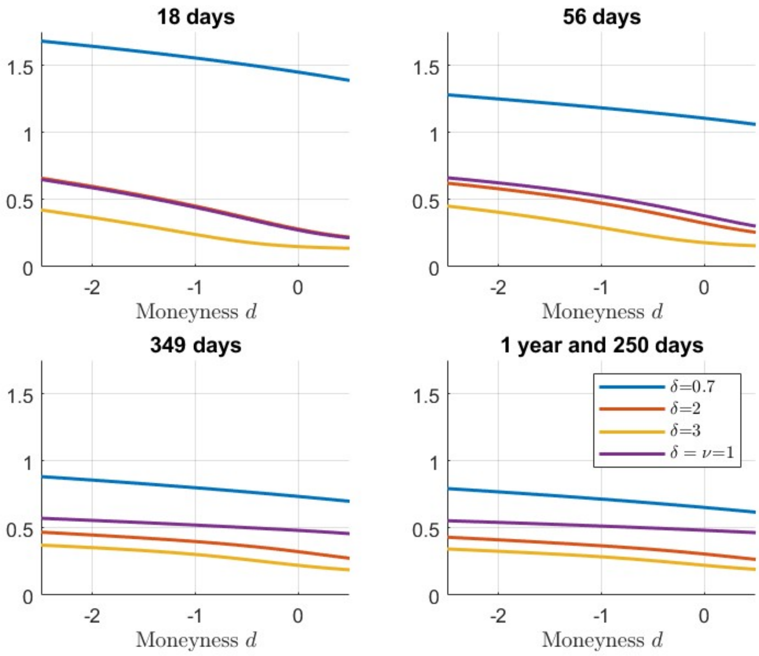

Figure 5: Impact of the parameter δ of the generalized Mittag-Leffler on the implied volatility. All others parameters as in Table 3, S&P500 case. Standardized moneyness: $d = \ln(K/S)/(\sigma_I\sqrt{T})$, as in Foresi and Wu (2005).

Finally, by means of Proposition 3 we can analyse the impact on the implied volatility of the GML model parameters ν and δ which primarily control the decay rate of the indices of skewness and excess kurtosis, as shown in section 2.3. In the interest of a realistic portray of the quantities of interest, we use model parameters consistent with option market quotes (indeed we use the parameters obtained from the model calibration performed in section 4).

In Figure 3, we plot the skewness and the excess kurtosis of the compound GML renewal diffusion process for the different values of ν (top panels) and δ (bottom panels). In Figures 4 and 5, we plot the implied volatilities generated by the same combination of parameters against the standardized moneyness

$$d = \frac{\ln(K/S)}{\sigma_I \sqrt{T}},$$

(see Carr and Wu, 2003, Foresi and Wu, 2005, for example). Such moneyness measure expresses the number of standard deviations that the log strike K is away from the log spot S; the scaling by the time to maturity T allows comparison across maturities, whilst the scaling by σ_I allows comparison across securities. The term σ_I represents a mean volatility level for each equity index, proxyed by the sample average of the implied volatility quotes underlying each equity index. We also plot the same quantities obtained from the Merton jump diffusion model, i.e. $\delta = \nu = 1$, with all the other parameters kept constant.

In Figure 3, we observe that in general the log-returns distribution generated by the GML model is more negatively skewed and leptokurtic than the one of the classical Merton jump diffusion model. Furthermore, as ν increases the log-returns distributions become less asymmetric and leptokurtic; the implied volatility instead reduces in value, as the smirk has less pronounced slope and curvature, as shown in Figure 4. This is consistent with the intuition that the slope and curvature of the smirk reflect the skewness and excess kurtosis of the underlying log-returns distribution (see Backus *et al.*, 2004, Foresi and Wu, 2005, for example).

The impact of δ on the statistics of the log-returns distribution is reversed compared to ν at least over the short period of time. This is visible in terms of short maturities implied volatilities. Indeed, this is consistent with the considerations offered in section 2.3.

4 Calibration

In this section we test the performance of our model in reproducing option implied volatility surfaces by means of a number of experiments based on market data.

4.1 Data collection and experimental setting

We download from Refinitiv end of day market prices on March 3, 2023 for European options written on four major international financial indices: Euro Stoxx, FTSE100, MIB and S&P500. We use out-of-the-money call and put options with maturities up to almost 2 years. Options with time to maturities less than 10 days, ask prices less than or equal to the bid price, and bids less than 3/8 are excluded. To address liquidity concerns, for each time to maturity we calculate the average open interest, and remove options with open interest less than 20% of this average. Finally, for calibration purposes, a maturity is included if at least five calls and five puts remain. The final number of time to maturities and contracts is summarized in Table 2. As a standard practice, SVI (Gatheral and Jacquier, 2014) is applied to obtain arbitrage free surfaces, if necessary. The term structure of discount rates is recovered implicitly from the put-call parity.

Table 2: Financial indices: number of time to maturities and total number of contracts considered in the calibration exercise.

Index	Maturities	Contracts
Euro Stoxx	12	531
FTSE 100	5	227
MIB	7	113
S&P500	9	614

For the purpose of model calibration, we define the error function

$$\epsilon(\theta, K_i, T_i) = \frac{ivol_{market}(K_i, T_i) - ivol_{model}(K_i, T_i; \theta)}{ivol_{market}(K_i, T_i)} \tag{12}$$

where $ivol_{market}(K_i, T_i)$ is the end of day market implied volatility for a contract struck at K_i and expiring at T_i, and $ivol_{model}(K_i, T_i; \theta)$ denotes the corresponding implied volatility originated by the model specification with parameter set θ under consideration. The calibration problem is stated as

$$\min_{\theta} \sum_{i=1}^{M} \epsilon(\theta, K_i, T_i)^2, \tag{13}$$

with θ within the parameter limits of the chosen model, and M denoting the total number of contracts.

In the following, we compare the performance of our construction for the several inter-arrival distributions reported in Table 1, bearing in mind that for the case of the exponential distribution our model returns the classical Merton (1976) jump diffusion model, as already noted in previous sections. The calibration performance is measured by the root mean square error

$$RMSE = \sqrt{\frac{1}{M} \sum_{i=1}^{M} \epsilon(\theta^*, K_i, T_i)^2},$$

with θ^* denoting the calibrated parameter set, and by the contribution given by each maturity slice

$$\frac{1}{M_T} \sum_{j=1}^{M_T} \epsilon(\theta^*, K_j, T)^2, \tag{14}$$

with M_T denoting the number of contracts with maturity T. Note that the performance measure (14) is calculated using the calibrated parameter set θ^* solution of the optimization problem (13), which uses all available strikes and maturities.

4.2 Results

The goals of the empirical exercise are to gauge the ability of the several specifications of our general setting in reproducing the full implied volatility surface, to understand the contribution in terms of improved performance offered by the Brownian motion, and to analyse the model behaviour across different time horizons.

In Table 3, we present the RMSEs together with the calibrated parameters obtained from our exercise. We consider the case in which the log-returns are driven by either the pure compound

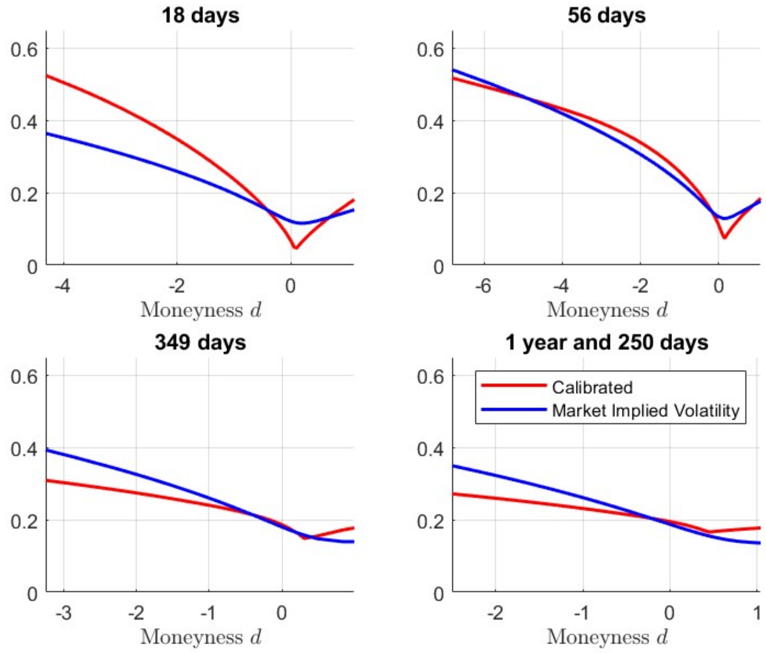

Figure 6: Calibration performance for the two shortest maturities, and for the ones closest to 1 and 2 years, S&P500: pure jump compound Poisson process ($\sigma = 0$ - exponentially distributed inter-arrival times). $RMSE = 0.1388$. Standardized moneyness: $d = \ln(K/S)/(\sigma_I \sqrt{T})$, as in Foresi and Wu (2005).

renewal process $Y(t)$ (and therefore σ is not calibrated and set to 0), or the compound renewal diffusion process $X(t)$.

Upon initial inspection, the impact of the diffusion term in reducing the RMSE is evident, as well as the benefit of replacing the exponential distribution with other distributions, notably the generalized Mittag-Leffler distribution, which demonstrates the best performance across all cases. In the following, in the interest of synthesis, we present only the calibration on the S&P500 options. Results for the other indices are available upon request.

4.2.1 The role of the diffusion component

In first instance, we quantify the contribution of the Brownian motion component. For illustration purposes, we consider the case of exponentially distributed inter-arrival times, i.e. the case in which the pure jump part is given by the compound Poisson process. The performances as measured by the RMSE are respectively 0.1388 and 0.0722. The added contribution of the Brownian motion component is evident.

Figures 6 and 7 illustrate the calibrated implied volatilities in correspondence of selected maturities as a function of the standardized moneyness d. In particular, we show in Figure 6 the case in which $\sigma = 0$ is set by default, and in Figure 7 the case in which $\sigma > 0$ is given by the calibration. These results highlight that the greatest improvement in adding the diffusion component is obtained in correspondence of short maturities. This is a reflection of the higher order moments 'tempering' effect that the Brownian motion offers as discussed in section 3.1.

In order to gain further insights, in Figure 8 we plot the error per maturity slice (14); panel a) in particular shows that the improvements due to adding the Brownian motion is common among all the maturities. Similar results hold for all inter-arrival distributions considered in this paper

Table 3: Calibration RMSE and calibrated parameters. For each model, top row: pure compound renewal risk driver $Y(t)$, bottom row: compound renewal diffusion risk driver $X(t)$. (*): calibrated Mittag-Leffler parameter $\nu = 1$, i.e. the resulting inter-arrival distribution coincides with the exponential one. (+): calibrated generalised Mittag-Leffler parameter $\nu = 1$, i.e. the resulting inter-arrival distribution coincides with the gamma one.

Renewal	log-returns	RMSE	σ	μ_Z	σ_Z	Renewal Parameters
				EUROSTOXX		
Exponential	$Y(t)$	0.1173	-	-0.0865	0.2016	$\lambda = 0.9413$
	$X(t)$	0.0846	0.0883	-0.1583	0.2793	$\lambda = 0.3794$
Gamma	$Y(t)$	0.1173	-	-0.0864	0.2014	$\delta = 0.9956, \lambda = 0.9346$
	$X(t)$	0.0826	0.0909	-0.1654	0.2816	$\delta = 1.0856, \lambda = 0.4465$
Weibull	$Y(t)$	0.1173	-	-0.0863	0.2015	$\lambda = 1.0728, k = 0.9901$
	$X(t)$	0.0823	0.0907	-0.1650	0.2819	$\lambda = 2.4619, k = 1.0614$
Noncentral chi-squared	$Y(t)$	0.1278	-	-0.1002	0.2465	$k = 1.7569, \lambda = 0.0000$
	$X(t)$	0.0826	0.0908	-0.1650	0.2811	$k = 2.1712, \lambda = 0.2388$
Inverse Gaussian	$Y(t)$	0.1418	-	-0.0692	0.1580	$\mu = 1.5767, \lambda = 0.2862$
	$X(t)$	0.1110	0.0946	-0.1347	0.2207	$\mu = 3.3166, \lambda = 0.8199$
Mittag-Leffler	$Y(t)$	0.1172	-	-0.0865	0.2023	$\lambda = 0.9220, \nu = 0.9874$
	$X(t)$	0.0846	0.0883	-0.1583	0.2794	$\lambda = 0.3793, \nu = 1.0000$ (*)
Generalised Mittag-Leffler	$Y(t)$	0.1144	-	-0.0856	0.1997	$\delta = 1.8326, \lambda = 1.8895, \nu = 0.7192$
	$X(t)$	0.0798	0.0900	-0.1625	0.2760	$\delta = 2.3990, \lambda = 1.3270, \nu = 0.6135$
				FTSE 100		
Exponential	$Y(t)$	0.1037	-	-0.0805	0.1909	$\lambda = 0.7011$
	$X(t)$	0.0858	0.0382	-0.1035	0.2271	$\lambda = 0.4741$
Gamma	$Y(t)$	0.1032	-	-0.0802	0.1902	$\delta = 1.0319, \lambda = 0.7592$
	$X(t)$	0.0829	0.0403	-0.1046	0.2260	$\delta = 1.0813, \lambda = 0.5754$
Weibull	$Y(t)$	0.1030	-	-0.0802	0.1905	$\lambda = 1.3810, k = 1.0160$
	$X(t)$	0.0827	0.0402	-0.1045	0.2262	$\lambda = 1.9034, k = 1.0584$
Noncentral chi-squared	$Y(t)$	0.1087	-	-0.0915	0.2165	$k = 1.8959, \lambda = 0.0000$
	$X(t)$	0.0835	0.0420	-0.1105	0.2373	$k = 2.1155, \lambda = 0.0000$
Inverse Gaussian	$Y(t)$	0.1520	-	-0.1009	0.2128	$\mu = 3.3888, \lambda = 0.7242$
	$X(t)$	0.1112	0.0502	-0.1093	0.1946	$\mu = 3.4982, \lambda = 0.7758$
Mittag-Leffler	$Y(t)$	0.1037	-	-0.0805	0.1910	$\lambda = 0.7010, \nu = 1.0000$ (*)
	$X(t)$	0.0858	0.0382	-0.1035	0.2271	$\lambda = 0.4741, \nu = 1.0000$ (*)
Generalised Mittag-Leffler	$Y(t)$	0.1002	-	-0.0791	0.1925	$\delta = 2.1674, \lambda = 1.7131, \nu = 0.6329$
	$X(t)$	0.0788	0.0398	-0.1032	0.2249	$\delta = 2.7209, \lambda = 1.7353, \nu = 0.5665$
				MIB		
Exponential	$Y(t)$	0.1549	-	-0.0965	0.2481	$\lambda = 0.7588$
	$X(t)$	0.0895	0.1324	-0.3892	0.3880	$\lambda = 0.1391$
Gamma	$Y(t)$	0.1480	-	-0.1438	0.3036	$\delta = 0.7076, \lambda = 0.2218$
	$X(t)$	0.0796	0.1253	-0.2759	0.3272	$\delta = 1.0032, \lambda = 0.1981$
Weibull	$Y(t)$	0.1542	-	-0.0969	0.2492	$\lambda = 1.3858, k = 0.9633$
	$X(t)$	0.0920	0.1277	-0.3151	0.3644	$\lambda = 4.6767, k = 1.0870$
Noncentral chi-squared	$Y(t)$	0.1569	-	-0.1130	0.2821	$k = 1.8201, \lambda = 0.0000$
	$X(t)$	0.0921	0.1280	-0.3196	0.3697	$k = 2.0658, \lambda = 2.1264$
Inverse Gaussian	$Y(t)$	0.1818	-	-0.1081	0.2976	$\mu = 3.2450, \lambda = 0.7779$
	$X(t)$	0.1293	0.1103	-0.1437	0.2277	$\mu = 3.3478, \lambda = 0.8372$
Mittag-Leffler	$Y(t)$	0.1540	-	-0.0968	0.2490	$\lambda = 0.7280, \nu = 0.9642$
	$X(t)$	0.0895	0.1324	-0.3892	0.3880	$\lambda = 0.1391, \nu = 1.0000$ (*)
Generalised Mittag-Leffler	$Y(t)$	0.1480	-	-0.1438	0.3036	$\delta = 0.7076, \lambda = 0.2218, \nu = 1.0000$ (+)
	$X(t)$	0.0796	0.1253	-0.2759	0.3272	$\delta = 1.0032, \lambda = 0.1981, \nu = 1.0000$ (+)
				S&P500		
Exponential	$Y(t)$	0.1388	-	-0.0948	0.1839	$\lambda = 1.0757$
	$X(t)$	0.0722	0.1175	-0.3361	0.2639	$\lambda = 0.2078$
Gamma	$Y(t)$	0.1388	-	-0.0947	0.1844	$\delta = 0.9920, \lambda = 1.0560$
	$X(t)$	0.0678	0.1161	-0.3166	0.2468	$\delta = 1.1696, \lambda = 0.3523$
Weibull	$Y(t)$	0.1387	-	-0.0941	0.1843	$\lambda = 0.9411, k = 0.9876$
	$X(t)$	0.0671	0.1184	-0.3469	0.2487	$\lambda = 3.7943, k = 1.1220$
Noncentral chi-squared	$Y(t)$	0.1506	-	-0.1169	0.2341	$k = 1.6851, \lambda = 0.0000$
	$X(t)$	0.0676	0.1171	-0.3299	0.2479	$k = 2.2957, \lambda = 1.0544$
Inverse Gaussian	$Y(t)$	0.1582	-	-0.0726	0.1651	$\mu = 2.1519, \lambda = 0.2974$
	$X(t)$	0.0892	0.1008	-0.1777	0.1979	$\mu = 3.8014, \lambda = 0.8470$
Mittag-Leffler	$Y(t)$	0.1386	-	-0.0933	0.1844	$\lambda = 1.0577, \nu = 0.9827$
	$X(t)$	0.0722	0.1175	-0.3361	0.2639	$\lambda = 0.2077, \nu = 1.0000$ (*)
Generalised Mittag-Leffler	$Y(t)$	0.1367	-	-0.0897	0.1785	$\delta = 1.5791, \lambda = 1.8785, \nu = 0.7810$
	$X(t)$	0.0624	0.1200	-0.3460	0.2465	$\delta = 3.7803, \lambda = 1.6166, \nu = 0.4984$

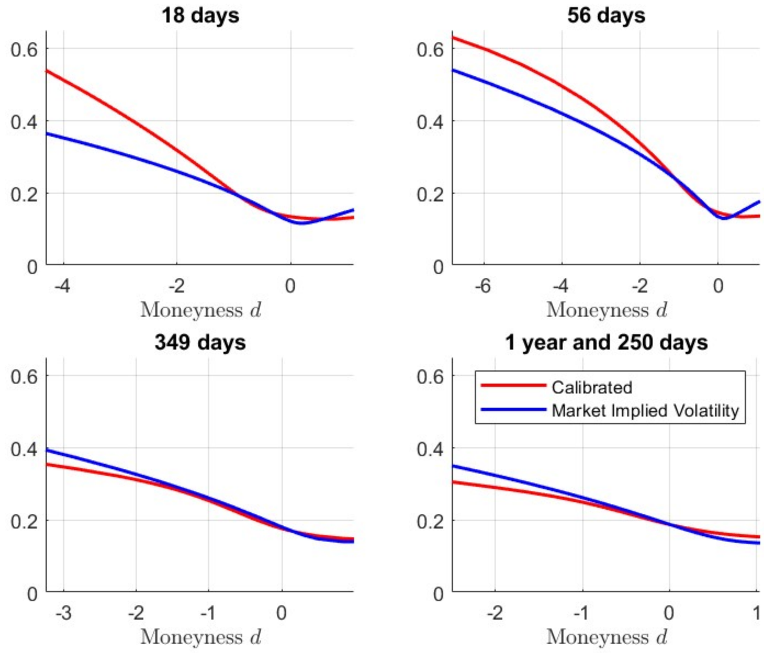

Figure 7: Calibration performance for the two shortest maturities, and for the ones closest to 1 and 2 years, S&P500: jump diffusion compound Poisson process (σ calibrated - exponentially distributed inter-arrival times). $RMSE = 0.0722$. Standardized moneyness: $d = \ln(K/S)/(\sigma_I\sqrt{T})$, as in Foresi and Wu (2005).

and are available upon request. Given these findings, in the following we consider the case $\sigma > 0$ only.

4.2.2 Renewal processes

Table 3 shows the benefit of replacing the exponential distribution with other distributions, notably the generalized Mittag-Leffler distribution, which demonstrates the best performance across all cases. A very close second best is given by both the gamma and the Weibull distributions. From Panel b) of Figure 8, we can observe that the improvement offered by the generalised Mittag-Leffler construction with respect to the Merton jump diffusion model is mainly on the short maturities: the model is therefore able to perform a good fit on the short maturities without losing accuracy on replicating the implied volatility surface on the long ones. In particular, from Table 3 we note the calibrated value of the parameter ν in the compound GML renewal diffusion process, which is always greater than 0.5, signalling a non vanishing long term implied volatility smirk, with the only exception of the S&P500 index, in which case the calibrated value is very close to the 0.5 threshold.

Looking at the resulting (unit time) mean and variance of the renewal process in Table 4, we observe that market option prices imply positive duration dependence except in the case of the ML model, which can only cater for negative duration dependence (see Jose and Abraham, 2011, for example). This could explain the fact that the calibration returns $\nu = 1$, i.e. equidispersion.

In Figure 9 we portray the calibrated probability of the generalised Mittag-Leffler renewal process at time 1 year and 3 years respectively. Figure 10 presents the resulting renewal function denoted as $m(t) = \mathbb{E}(N(t))$. Although for the exponential distribution the renewal function exhibits linearity, as $m(t) = \lambda t$, Figure 10 unequivocally demonstrates that this linearity does not

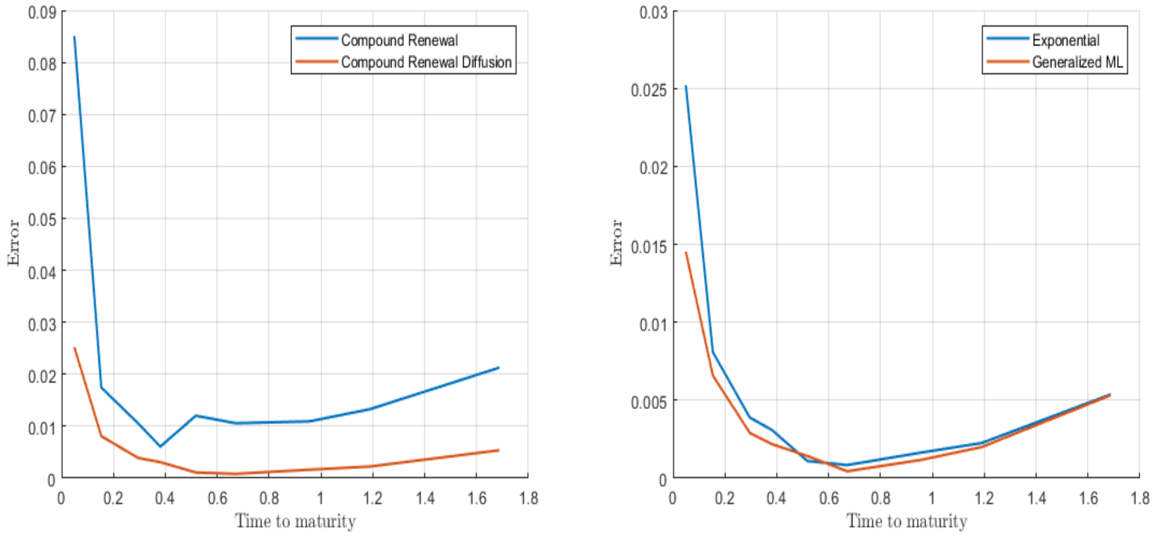

a) Exponential b) Exponential vs GML

Figure 8: Calibration performance per maturity slice. Error: $\sum_{j=1}^{M_T} \epsilon(\theta^*, K_j, T)^2 / M_T$ (see Equation (14)). Exponentially distributed inter-arrival times vs generalised Mittag-Leffler distributed inter-arrival times. Panel a): Role of the diffusion coefficient in the Exponential case. Panel b): Performance of the Exponential/Poisson jump diffusion model vs the GML compound renewal diffusion. Parameters: Table 3 for S&P500.

Table 4: Dispersion properties of the renewal distribution and first inter-arrival time. *VMR*: Variance-to-Mean ratio of the renewal process (see section 2.2). Parameters: Table 3 for the S&P500.

	$\mathbb{E}(N(1))$	$\mathbb{V}ar(N(1))$	VMR
Exponential	0.208	0.208	1.000
Gamma	0.253	0.245	0.971
Weibull	0.221	0.216	0.976
Noncentral chi-squared	0.238	0.232	0.972
Inverse Gaussian	0.582	0.535	0.920
Mittag-Leffler	0.208	0.208	1.000
Generalised Mittag-Leffler	0.214	0.214	0.999

hold true for the generalised Mittag-Leffler distribution.

Finally, Figure 11 shows the distribution of the inter-arrival times: whilst the exponential one (which coincides with the Mittag-Leffler) is monotone, all the others are increasing and then decreasing, confirming the superiority of unimodal distributions in terms of flexibility for calibration purposes. The only noticeable exception is the inverse Gaussian distribution, which shows a different scale with respect to the others: this distribution seems not flexible enough to capture the market information properly, resulting in the worst calibration performance, as shown in Table 3.

4.2.3 Pricing exotic options

As a further analysis, we examine Up & Out put options on forwards with a maturity of 349 days and a strike of 3325. Prices are computed by Monte Carlo simulation based on the pseudocode 1 offered in section 2.4, leveraging the Antithetic Variates technique for variance reduction. The

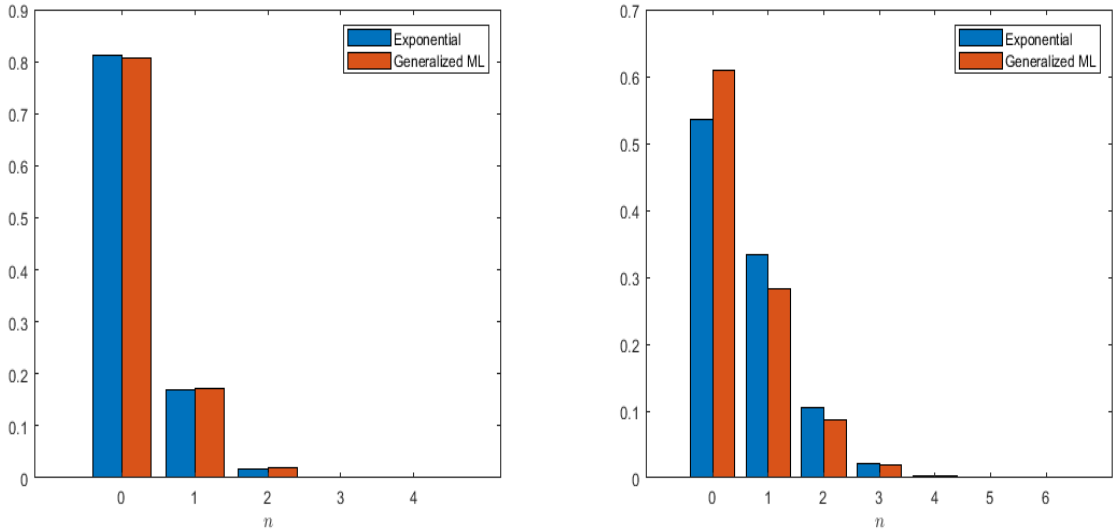

a) $\mathbb{P}(N(1) = n)$ b) $\mathbb{P}(N(3) = n)$

Figure 9: Calibrated distribution of the generalised Mittag-Leffler renewal process and Poisson process. Parameters: Table 3 for the S&P500.

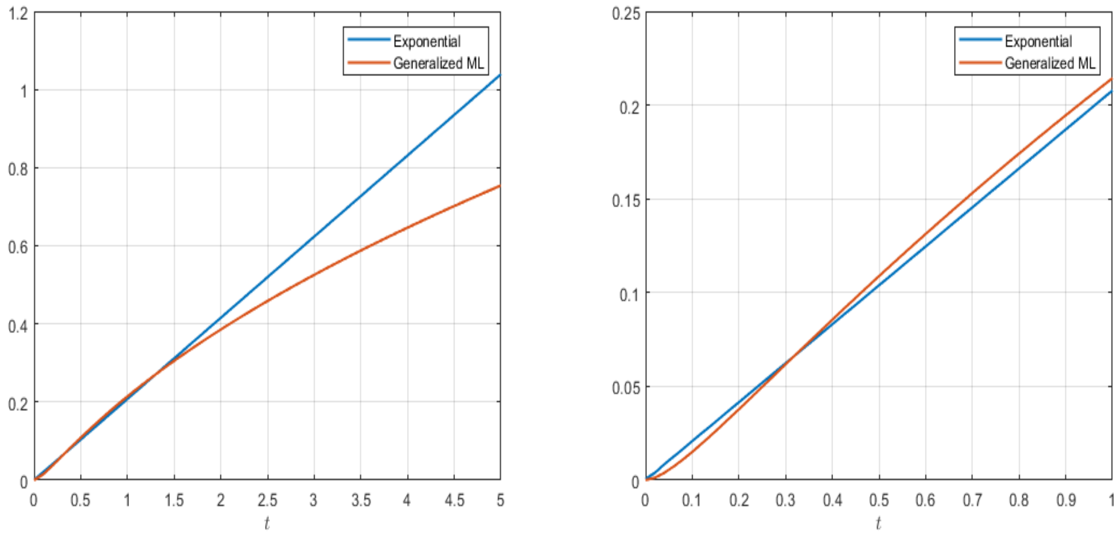

a) Renewal function   b) Zoom

Figure 10: The renewal function $m(t) = \mathbb{E}(N(t))$ for different time horizons (time in years). Parameters: Table 3 for the S&P500.

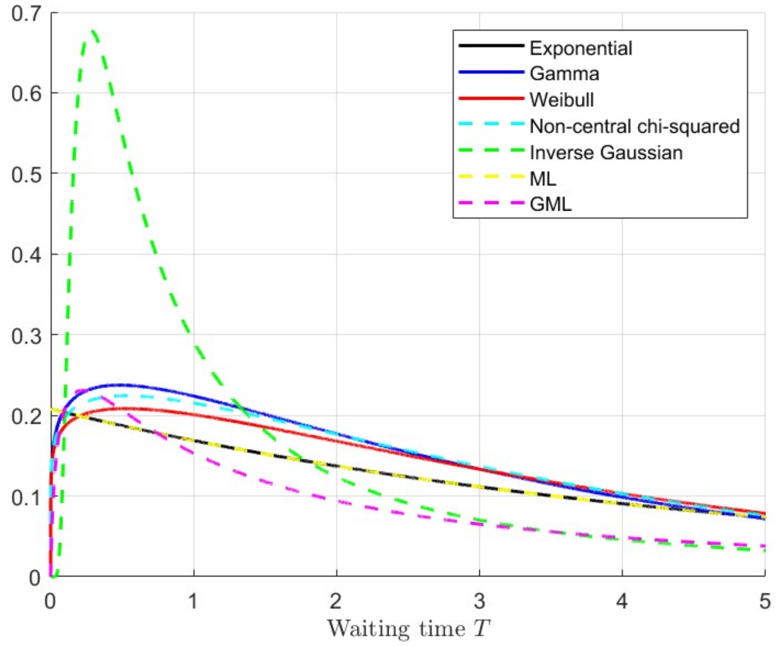

Figure 11: Calibrated distribution of the inter-arrival times. Parameters: Table 3 for S&P500.

Table 5: Up&Out put option pricing with upper barrier U. Maturity: 349 days. Strike: 3325. Forward price: 4276.59. Risk-free interest rate: 4.80%. Market price for the European Call: 988.20. Calibrated price for the exponential distribution (generalised Mittag-Leffler): 985.20 (987.88). $Price_E$ ($Price_{GML}$): barrier option price assuming the exponential (generalised Mittag-Leffler) distribution. Monte Carlo simulation with Antithetic Variates. N. simulation: 10^7 with monthly monitoring.

U	4300	4350	4400	4450	4500	4750	5000
$Price_E$	57.49	84.16	116.30	152.90	193.06	417.93	630.16
$Price_{GML}$	56.02	81.32	111.61	146.19	184.26	400.70	611.50
$\frac{\lvert Price_E - Price_{GML}\rvert}{Price_{GML}}$	2.62%	3.49%	4.20%	4.59%	4.78%	4.30%	3.05%

precise computation of the CDF using the Hilbert transform enables us to simulate inter-arrival times by employing numerical inversion and uniformly distributed random variables.

We compare the option prices derived from two different models: the one based on the exponential distribution for the inter-arrival times and the best model, which is built on the generalised Mittag-Leffler distribution.

From Table 5, it is evident that the maximum pricing error when using the exponential distribution, rather than the generalised Mittag-Leffler distribution, is 4.78%, with an average error across the entire table amounting to 3.86%. In contrast, for the calibrated European call options with the same maturity and strike, the error is merely 0.27%. This discrepancy underscores the substantial impact of the counting process on the pricing of path-dependent derivatives.

5 Conclusions

We have developed an option pricing model based on renewal processes, with the aim of studying the impact of the choice of the underlying inter-arrival distribution on the fit to market volatility surfaces. The proposed setting offers a simple and intuitive formula for the price of European vanilla options which is analytical up to an infinite summation, and a fast and immediate Monte Carlo simulation procedure for exotic options. The implementation of both is based on the Hilbert transform for the recovery of the probability function of the resulting counting process; this allows us to compute the key quantities in analytical form.

The results from the empirical study based on market quotes for options written on major indices show that the best fit is achieved with a log-returns dynamics which includes both a Brownian motion and a compound renewal process whose inter-arrival times are distributed according to the generalised Mittag-Leffler distribution. Thus, the log-returns process shows finite mean and variance (in contrast to the log-stable model of Carr and Wu, 2003) but non-vanishing skewness and excess kurtosis over the time horizons; furthermore, based on the calibrated parameters, its discontinuous part is characterised by a distribution of both the inter-arrival times and the counting process which is under-dispersed. In other words, the number of trades captured by the renewal process is more regular than in the case of the Poisson process, denoting positive duration dependence.

The option pricing formula also formalizes analytically the positive relation between the log-returns distribution implied volatility and the number of trades occurring in the given period. As the latter are no longer modelled by a process with independent and stationary increments, we can better capture the behaviour of the implied volatility across the several tenors, and gain interesting insights into the generation of stochastic volatility behaviours.

Acknowledgments

The Authors would like to thank two anonymous referees for their valuable comments. This work has been presented at the WQF2023 Conference in Gaeta, the 2nd Quantitative Finance Conference in London, the Quant Insights Conference: Black-Scholes 50th Anniversary (online), and QuantMinds International 2023 in London. We are grateful to the participants for their useful comments and suggestions. Usual cavet applies.

- No potential competing interest was reported by the authors.
- No funding was received

References

Backus, D.K., Foresi, S. and Wu, L., Accounting for biases in Black-Scholes. *SSRN Electronic Journal*, 2004.

Ballotta, L., Eberlein, E. and Rayée, G., Time changes, Fourier transforms and the joint calibration to the S&P500/VIX smiles. *Preprint*, 2023.

Ballotta, L. and Rayée, G., Smiles & smirks: Volatility and leverage by jumps. *European Journal of Operational Research*, 2022, **298**, 1145–1161.

Barndorff-Nielsen, O.E., Processes of normal inverse Gaussian type. *Finance and Stochastics*, 1997, **2**, 41–68.

Beghin, L. and Orsingher, E., Poisson-type processes governed by fractional and higher-order recursive differential equations. *Electronic Journal of Probability*, 2010, **15**.

Black, F. and Scholes, M., The pricing of options and corporate liabilities. *Journal of Political Economy*, 1973, **81**, 637–654.

Cahoy, D.O. and Polito, F., Renewal processes based on generalized Mittag–Leffler waiting times. *Communications in Nonlinear Science and Numerical Simulation*, 2013, **18**, 639–650.

Cai, N. and Kou, S.G., Option pricing under a mixed-exponential jump diffusion model. *Management Science*, 2011, **57**, 2067–2081.

Capelas de Oliveira, E., Mainardi, F. and Vaz, J., Models based on Mittag-Leffler functions for anomalous relaxation in dielectrics. *The European Physical Journal Special Topics*, 2011, **193**, 161–171.

Carr, P., Geman, H., Madan, D.B. and Yor, M., Stochastic volatility for Lévy processes. *Mathematical Finance*, 2003, **13**, 345–382.

Carr, P. and Wu, L., The finite moment log stable process and option pricing. *Journal of Finance*, 2003, **58**, 753–777.

Carr, P. and Wu, L., Time-changed Lévy processes and option pricing. *Journal of Financial Economics*, 2004, **71**, 113–141.

Cartea, Á., Derivatives pricing with marked point processes using tick-by-tick data. *Quantitative Finance*, 2013, **13**, 111–123.

Cartea, Á. and Meyer-Brandis, T., How duration between trades of underlying securities affects option prices. *Review of Finance*, 2009, **14**, 749–785.

Clark, P.K., A subordinated stochastic process model with finite variance for speculative prices. *Econometrica*, 1973, **41**, 135–155.

Eberlein, E., Keller, U. and Prause, K., New insights into smile, mispricing, and Value at Risk: The hyperbolic model. *The Journal of Business*, 1998, **71**, 371–405.

Eberlein, E., Glau, K. and Papapantoleon, A., Analysis of Fourier transform valuation formulas and applications. *Applied Mathematical Finance*, 2010, **17**, 211–240.

Eberlein, E. and Keller, U., Hyperbolic distributions in finance. *Bernoulli*, 1995, **1**, 281–299.

Engle, R.F., The econometrics of ultra-high-frequency data. *Econometrica*, 2000, **68**, 1–22.

Engle, R.F. and Russell, J.R., Autoregressive conditional duration: A new model for irregularly spaced transaction data. *Econometrica*, 1998, **66**, 1127–1162.

Feng, L. and Lin, X., Inverting analytic characteristic functions and financial applications. *SIAM Journal on Financial Mathematics*, 2013, **4**, 372–398.

Feng, L. and Linetsky, V., Pricing discretely monitored barrier options and defaultable bonds in Lévy process models: A fast Hilbert transform approach. *Mathematical Finance*, 2008, **18**, 337–384.

Foresi, S. and Wu, L., Crash–O–Phobia: A domestic fear or a worldwide concern?. *The Journal of Derivatives*, 2005, **13**, 8–21.

Fusai, G., Germano, G. and Marazzina, D., Spitzer identity, Wiener-Hopf factorization and pricing of discretely monitored exotic options. *European Journal of Operational Research*, 2016, **251**, 124–134.

Gatheral, J. and Jacquier, A., Arbitrage-free SVI volatility surfaces. *Quantitative Finance*, 2014, **14**, 59–71.

Gut, A., *Stopped Random Walks. Limit Theorems and Applications*, 1988 (Springer: New York).

Heston, S., A closed-form solution for options with stochastic volatility with applications to bond and currency options. *The Review of Financial Studies*, 1993, **6**, 327–343.

Huang, J.Z. and Wu, L., Specification analysis of option pricing models based on time-changed Lévy processes. *Journal of Finance*, 2004, **59**, 1405–1439.

Huillet, T.E., On Mittag-Leffler distributions and related stochastic processes. *Journal of Computational and Applied Mathematics*, 2016, **296**, 181–211.

Jacquier, A. and Torricelli, L., Anomalous diffusions in option prices: connecting trade duration and the volatility term structure. *SIAM Journal on Financial Mathematics*, 2020, **11**, 1137–1167.

Jones, C.M., Kaul, G. and Lipson, M.L., Transactions, volume, and volatility. *Review of Financial Studies*, 1994, **7**, 631–651.

Jose, K.K. and Abraham, B., A count model based on Mittag-Leffler interarrival times. *Statistica*, 2011, **71**, 501–514.

Kou, S.G., A jump-diffusion model for option pricing. *Management Science*, 2002, **48**, 1086–1101.

Lemeshko, B.Y., Lemeshko, S.B., Akushkina, K.A., Nikulin, M.S. and Saaidia, N., Inverse Gaussian model and its applications in reliability and survival analysis. In *Mathematical and Statistical Models and Methods in Reliability*, edited by V. Rykov, N. Balakrishnan and M. Nikulin, pp. 433–453, 2010 (Birkhäuser: Boston, MA).

Madan, D.B., Carr, P. and Chang, E., The Variance Gamma process and option pricing. *European Finance Review*, 1998, **2**, 79–105.

Mainardi, F., Raberto, M., Gorenflo, R. and Scalas, E., Fractional calculus and continuous-time finance II: The waiting-time distribution. *Physica A: Statistical Mechanics and its Applications*, 2000, **287**, 468–481.

Mathai, A.M., Saxena, R.K. and Haubold, H.J., *The H-function: Theory and Applications*, 2009 (Springer Science & Business Media: New York, NY).

McShane, B., Adrian, M., Bradlow, E.T. and Fader, P.S., Count models based on Weibull inter-arrival times. *Journal of Business & Economic Statistics*, 2008, **26**, 369–378.

Merton, R.C., Option pricing when underlying stock returns are discontinuous. *Journal of Financial Economics*, 1976, **3**, 125–144.

Michelitsch, T.M. and Riascos, A.P., Generalized fractional Poisson process and related stochastic dynamics. *Fractional Calculus and Applied Analysis*, 2020, **23**, 656–693.

Montero, M., Renewal equations for option pricing. *The European Physical Journal B*, 2008, **65**, 295–306.

Niki, N., Shigekazu, N. and Inoue, H., Cumulants of random sum distributions. *Communications in Statistics - Theory and Methods*, 1990, **19**, 1857–1861.

Pillai, R.N., On Mittag-Leffler functions and related distributions. *Annals of the Institute of Statistical Mathematics*, 1990, **42**, 157–161.

Prabhakar, T.R., A singular integral equation with a general Mittag–Leffler function in the kernel. *Yokohama Mathematical Journal*, 1971, **19**, 7–15.

Ross, S., *Applied Probability Models with Optimization Applications*, 1970 (Holden–Day, Inc.: San Francisco).

Ross, S.A., Information and volatility: The no-arbitrage martingale approach to timing and resolution irrelevancy. *The Journal of Finance*, 1989, **44**, 1–17.

Scalas, E., Gorenflo, R. and Mainardi, F., Fractional calculus and continuous-time finance. *Physica A: Statistical Mechanics and its Applications*, 2000, **284**, 376–384.

Smith, W.L., On the cumulants of renewal processes. *Biometrika*, 1959, **46**, 1.

Winkelmann, R., Duration dependence and dispersion in count-data models. *Journal of Business & Economic Statistics*, 1995, **13**, 467–474.

Xue, Y., Gençay, R. and Fagan, S., Jump detection with wavelets for high-frequency financial time series. *Quantitative Finance*, 2013, **14**, 1427–1444.

Yannaros, N., On Cox processes and gamma renewal processes. *Journal of Applied Probability*, 1988, **25**, 423–427.

Yannaros, N., Weibull renewal processes. *Annals of the Institute of Statistical Mathematics*, 1994, **46**, 641–648.

A Appendix: Proofs

A.1 Proof of Proposition 2

i) We first consider the probability generating function of the renewal counting process

$$G_{N(t)}(u) = \mathbb{E}\left(u^{N(t)}\right) = \sum_{n=0}^{\infty} u^n \mathbb{P}(N(t) = n), \quad |u| \leq 1, \tag{A.1}$$

which in the case of the Mittag-Leffler distribution, i.e. for $\delta = 1$, has analytical expression

$$G_{N(t)}(u) = E_\nu\left(\lambda t^\nu (u-1)\right).$$

By straightforward differentiation (and setting $u = 1$) of the above, we can obtain the factorial moments (see Huillet, 2016, for example)

$$\mathbb{E}\left((N(t))_k\right) = m_k t^{k\nu}$$

with $(x)_k$ denoting the falling factorial, i.e.

$$(x)_k = \underbrace{x(x-1)(x-2)\cdots(x-k+1)}_{k \text{ terms}}.$$

The raw moments of $N(t)$ can now be recovered from the factorial ones using the known relationship

$$\mathbb{E}\left(N(t)^k\right) = \sum_{j=0}^{k} \mathcal{S}(j,k)\mathbb{E}\left((N(t))_k\right),$$

with $\mathcal{S}(j,k)$ denoting the Stirling numbers of the second kind. We recall also the relationship between raw moments and cumulants

$$\begin{aligned}
c_1(N(t)) &= \mathbb{E}(N(t)) \\
c_2(N(t)) &= \mathbb{E}\left(N(t)^2\right) - \mathbb{E}(N(t))^2 \\
c_3(N(t)) &= \mathbb{E}\left(N(t)^3\right) - 3\mathbb{E}\left(N(t)^2\right)\mathbb{E}(N(t)) + 2\mathbb{E}(N(t))^3 \\
c_4(N(t)) &= \mathbb{E}\left(N(t)^4\right) - 4\mathbb{E}\left(N(t)^3\right)\mathbb{E}(N(t)) + 6\mathbb{E}\left(N(t)^2\right)\mathbb{E}(N(t))^2 \\
&\quad -3\mathbb{E}(N(t))^4 - 3c_2(N(t))^2,
\end{aligned}$$

from which it follows that the first four cumulants of the renewal process $N(t)$ are

$$\begin{aligned}
c_1(N(t)) &= t^\nu m_1 \\
c_2(N(t)) &= t^{2\nu}\left(m_2 - m_1^2\right) + t^\nu \mu_2 \\
c_3(N(t)) &= t^{3\nu}\left(m_3 - 3m_2 m_1 + 2m_1^3\right) + 3t^{2\nu}(m_2 - m_1^2) + t^\nu m_1 \\
c_4(N(t)) &= t^{4\nu}(m_4 - 4m_1 m_3 + 6m_1^2 m_2 - 3m_1^4) + 6t^{3\nu}(m_3 - 2m_1 m_2 + m_1^3) \\
&\quad +t^{2\nu}(7m_2 - 4m_1^2) + t^\nu m_1 - 3c_2(N(t))^2.
\end{aligned}$$

The stated result then follows from equations (4)–(7).

ii) The result follows by observing that when taking the limit for $t \to \infty$ the only terms of relevance are the ones containing the highest power of t^{ν}.

iii) For small t, $c_2 \sim t^{\nu}\mu_2 m_1$, $c_3 \sim t^{\nu}\mu_3 m_1$ and $c_4 \sim t^{\nu}\mu_4 m_1 - 3c_2(t)^2$, from which the result follows.

A.2 The asymptotic moments of the compound GML renewal process

Although, in the GML case the cumulants of the process $Y(t)$ cannot be recovered analytically, useful information can be obtained from the Laplace transform of the probability generating function of the associated renewal process $N(t)$ by extending an argument of Michelitsch and Riascos (2020) based on Tauberian theorems.

In details, the Laplace transform of (A.1) is

$$\mathcal{L}\left(G_{N(t)}(u)\right)(s) = \frac{1 - \mathcal{L}\left(f(t)\right)(s)}{s(1 - u\mathcal{L}\left(f(t)\right)(s))}.$$

By repeated differentiation with respect to u (and setting $u = 1$), it follows that the Laplace transform of the factorial moment of order $k \in \mathbb{N}$ of the renewal process $N(t)$ is

$$\mathcal{L}\left(\mathbb{E}\left((N(t))_k\right)\right)(s) = \frac{\Gamma(k+1)}{s\left(\left(1 + \frac{s^{\nu}}{\lambda}\right)^{\delta} - 1\right)^{k}}. \tag{A.2}$$

We note that for small values of s, i.e. for $|s| \to 0$,

$$\mathcal{L}\left(\mathbb{E}\left((N(t))_k\right)\right)(s) \approx \left(\frac{\lambda}{\delta}\right)^{k} \Gamma(k+1)s^{-\nu k-1},$$

from which the asymptotic behaviour for $t \to \infty$ of the factorial moments can be obtained as

$$\mathbb{E}\left((N(t))_k\right) \approx \left(\frac{\lambda}{\delta}\right)^{k} \frac{\Gamma(k+1)}{\Gamma(\nu k+1)} t^{\nu k}.$$

Following the same steps as in the proof of Proposition 2, we can verify that for $t \to \infty$ the asymptotic values of $sk(Y(t))$ and $ek(Y(t))$ coincide with the ones reported in Proposition 2.*ii*.

In order to deduce the behaviour for $t \to 0$, we need instead to consider large value of s in equation (A.2): for $|s| \to \infty$, indeed, we have

$$\mathcal{L}\left(\mathbb{E}\left((N(t))_k\right)\right)(s) \approx \Gamma(k+1)\lambda^{\delta k}s^{-\nu\delta k-1},$$

from which it follows that the asymptotic behaviour for $t \to 0$ of the factorial moments can be obtained as

$$\mathbb{E}\left((N(t))_k\right) \approx \frac{\Gamma(k+1)}{\Gamma(\nu k+1)}\lambda^{\delta k}t^{\nu\delta k}.$$

A.3 Proof of Proposition 3

From the definition of the stock price process in Equation (9), by conditioning on $N(T) = n \in \mathbb{N}$, and considering the sum of the n independent normally distributed random variables with mean

μ_Z and variance σ_Z^2, we deduce that

$$\ln \frac{S(T)}{S(0)} = (r - q)\, T - \varpi(T) + \sigma W(T) + n\mu_Z + \sqrt{n}\sigma_Z \zeta,$$

for $\zeta \sim \mathcal{N}(0,1)$, independent of the Brownian motion $W(T)$. Consequently,

$$\mathbb{V}ar \left(\ln \frac{S(T)}{S(0)} \right) = \sigma^2 T + n\sigma_Z^2 = v^2(n)T$$

for

$$v(n) = \sqrt{\sigma^2 + \frac{n}{T}\sigma_Z^2},$$

and

$$\ln \frac{S(T)}{S(0)}\bigg|_{N(T)=n} \sim \mathcal{N}\left(\left(r - q(n) - \frac{1}{2}v^2(n) \right) T, v^2(n)T \right)$$

for

$$q(n) = q + \frac{1}{T} \ln\, \phi_Y(-\mathrm{i}; T) - \frac{n}{T}\left(\mu_Z + \frac{\sigma_Z^2}{2} \right).$$

Let $B(T)$ be a Brownian motion, from the previous results it follows that, conditioned on $N(T) = n$, we can rewrite the stock price as

$$S(T) = S(0)e^{\left(r - q(n) - \frac{1}{2}v^2(n)\right)T + v(n)B(T)},$$

which is in the appropriate form for the application of the Black-Scholes formula to a price process with dividend yield $q(n)$ and volatility $v(n)$. The price of the option then follows by averaging over the distribution of the counting process $N(T)$.